



## On the Active Vibration Control of Nonlinear Uncertain Structures

Vasilis K. Dertimanis<sup>1</sup>, Eleni N. Chatzi<sup>1</sup>, Sami F. Masri<sup>2</sup>

<sup>1</sup> Institute of Structural Engineering, Department of Civil, Environmental and Geomatic Engineering, ETH Zurich,  
Stefano-Francini-Platz 5, Zurich, 8093, Switzerland, Emails: v.derti@ibk.baug.ethz.ch; chatzi@ibk.baug.ethz.ch

<sup>2</sup> Viterbi School of Engineering, University of Southern California, 3620 South Vermont Ave., Los Angeles, CA 90089, USA, Email: masri@usc.edu

Received June 15 2020; Revised November 09 2020; Accepted for publication November 09 2020.

Corresponding author: V.K. Dertimanis (v.derti@ibk.baug.ethz.ch)

© 2021 Published by Shahid Chamran University of Ahvaz

**Abstract.** This study proposes an active nonlinear control strategy for effective vibration mitigation in nonlinear dynamical systems characterized by uncertainty. The proposed scheme relies on the coupling of a Bayesian nonlinear observer, namely the Unscented Kalman Filter (UKF) with a two-stage control process. The UKF is implemented for adaptive joint state and parameter estimation, with the estimated states and parameters passed onto the controller. The controller comprises a first task of feedback linearization, allowing for subsequent integration of any linear control strategy, such as addition of damping, LQR control, or other, which then operates on the linearized state equations. The proposed framework is validated on a Duffing oscillator characterized by light damping and an uncertain nonlinear parameter under harmonic and stochastic disturbance. The demonstrated performance suggests that the proposed Bayesian approach offers a competitive approach for active vibration suppression in nonlinear uncertain systems.

**Keywords:** Vibration Mitigation, Nonlinear Adaptive Control, Unscented Kalman Filter, Linear-Quadratic Regulator, Joint State and Parameter Identification, State-feedback Linearization.

### 1. Introduction

A particular challenge in the domain of structural vibration control [1]-[4] lies in vibration attenuation of structures that feature nonlinear characteristics. Such structures, usually described by nonlinear differential equations of fixed parameters, are oftentimes further exposed to some degree of uncertainty [5]; in the sense that these parameters can be partially known, time-varying, or even completely unknown. This can be attributed to the inability of existing models to account for complex mechanisms, often relating to energy dissipation, or even the divergence of system properties from their design values due to aging, deterioration, environmental, or plasticity effects.

Within this context, the effective mitigation of vibration for nonlinear and uncertain systems calls for adoption of adaptive control schemes [6] that are able to account for variability of the system parameters, and more importantly do so, for systems whose intrinsic behavior is nonlinear. Such implementations are less commonly met in the field of structural vibration mitigation, where often a linear time-invariant assumption is placed on the structural behavior. Previous works in this direction include the fuzzy PID-type controller introduced by Guclu and Yazici [7] for the active control of a nonlinear structure by means of a tuned mass damper (ATMD), aiming to improve seismic performance. Ashour, O.N., Nayfeh [8] propose a nonlinear adaptive vibration absorber to control the vibrations of flexible structures. Adaptivity is ensured via incorporation of a frequency-measurement technique. In this sense, system identification enters the loop, related to the scheme introduced herein. Beyond active control, adaptivity has been explored in the context of semi-active control schemes [9], which are often preferred due to their potential to match the adaptability of the active class with lower power requirements. In a semi-active implementation, Bitaraf and Hurlebaus [10] propose an acceleration feedback-based control scheme, with a neural network used for the inverse model of the Magneto-Rheological (MR) damper control voltage, to suppress the detrimental effects of earthquakes on an MR-controlled tall building. Weber [11] proposes a control-oriented mapping approach to reduce modelling effort of the inverse MR damper behavior, which compensates for the main steady-state nonlinearity of the MR damper force and thereby linearizes the plant. A robust force-tracking control scheme is introduced to tackle the issue of model imperfections and parameter uncertainties by employing parallel proportional and integral feedback gains. Cetin et al. [12] employ nonlinear filters in conjunction with Lyapunov-based parameter estimators to compensate for uncertainties in both the structural system and the damper characteristics. The proposed controller has been experimentally validated on a six-degree-of-freedom structure, which is tested on a shake table. In this work adaptivity will rely on the fusion of a system identification technique with an appropriate control law.

For incorporation within the active control loop, the system identification task will need to be accomplished in real-time, while accommodating for nonlinearity and uncertainty. Therefore, schemes that can handle Joint State and Parameter Estimation (JS&PE) for nonlinear systems are necessary. In treating a problem of this nature, techniques relying on use of nonlinear Bayesian filters form the norm. This includes implementations with the Extended Kalman Filter (EKF) [12]-[14], the Unscented Kalman Filter (UKF) [13][15], as well as Sequential Monte Carlo or Particle Filter methods [16]-[19]. The UKF is a nonlinear variant of the Kalman Filter, made possible via use of the Unscented Transform (UT), which was introduced by Julier and Uhlmann [20], and forms an



improvement to the popularly used EKF method, which relies on linearization [21]-[23]. The UKF is the system identification tool adopted in this work [24]-[27].

Within the context of adaptive control, the UKF has previously been coupled with control strategies [28], particularly for the case of robotics applications. For the majority of these works, the UKF is primarily exploited as a state estimator. Marafioti [29] carries out a cross-assessment of UKF versus the EKF for model predictive control (MPC), with results favoring adoption of a UKF approach. Sunderhauf [30] draws a similar conclusion when employing the two for autonomous airship control. Wang [31] implements fuzzy control of nonlinear systems via use of the UKF as the nonlinear state estimator. In [32] control of an autoclave reactor is enforced via a UKF based multi-variable nonlinear model predictive control algorithm. Beyond estimation of dynamic states, the adoption of the UKF for additionally estimating the uncertain parameters of a nonlinear system is less common. Araki and Okada [33] exploit the UKF for parameter identification of an Acrobot system, which is then controlled via an energy-based approach, while Bisgaard et al. [34] utilize the UKF for identifying the slung load states of a helicopter system. Both works accomplish the parameter identification task separately to state estimation. The fusion of the UKF with a control approach under a joint state and parameter estimation scheme, for the purpose of structural vibration mitigation, remains less explored in existing literature [35], with a first step accomplished in previous work of the authoring team [36].

Under the assumption of measured states, a class of methods for nonlinear control relies on feedback linearization [37],[38]. The underlying concept is quite simple and aims at transforming a nonlinear system into a linear one, by adding a component to the control force that cancels the nonlinear dynamics. When this succeeds, the state equation becomes linear and classical control methods can be applied. This strategy is adopted in this work, while the Linear Quadratic Regulator (LQR) is selected as the control tool; a choice that proves popular for vibration mitigation purposes [39],[40]. The LQR controller requires full-state feedback, i.e., the estimation of the full vector of dynamical states. The direct measurement of the states is practically infeasible, due to obvious restrictions in terms of availability of sensors, but also due to limitations in the reachability of certain structural locations. To overcome this issue, the LQR is typically coupled with a state estimator. In the linear case, this results in the well-known Linear Quadratic Gaussian (LQG) control scheme [41],[42]. When however discussing adoption for nonlinear dynamical systems, this reasoning needs to be extended via adoption of nonlinear filters; a coupling which remains relatively less explored [43]-[46]. In this work, we explore coupling of an LQR with a nonlinear estimator, for the purpose of both state and parameter identification, thereby tackling systems which further to nonlinearity are compromised by uncertainty in their defining parameters.

The linear sub-problem, i.e., the treatment of a linear system with uncertain parameters, although still open to research, has been treated to a large extent, both in an active [47] and semi-active [48],[49] setting. In these previous works of the authors, it has been shown that the use of an appropriate Bayesian filter can effectively account for the presence of parametric uncertainties in real-time. The extension of this scheme to nonlinear systems is, nevertheless, non-trivial. This is mainly due to the additional complexity that is imposed by the nonlinear dynamics, which render the design of a controller a difficult task. We explore this problem and introduce an active nonlinear vibration control framework that is simple, straightforward and implementable in real-time. Following the results received for implementation in the linear case of vehicle vibration suppression [47], we propose the architecture of Fig. 1. The measured structural excitations and responses,  $\mathbf{u}_{d,k}$  and  $\mathbf{y}_k$ , respectively, are fed to an unscented Kalman filter (UKF), which is implemented for adaptive joint state and parameter estimation, while the estimated states  $\xi_k$  and parameters  $\theta$  are then forwarded to the controller.

The adopted control law comprises two tasks; firstly, application of feedback linearization for canceling the nonlinear dynamics of the system, which allows for subsequent adoption of any conventional linear control strategy on the linearized state equations, such as addition of damping, LQR control, etc. The combined control forces  $\mathbf{u}_{c,k}$  accordingly serve as additional excitations to the system, while are further “copied” to the UKF, in order to ensure consistency between the closed-loop dynamics and the Bayesian observer. The proposed framework is validated on a Duffing oscillator with light damping and uncertain nonlinear parameter. The transient and the steady-state behavior of the closed loop dynamics is investigated under harmonic and chirp disturbance, and we comment on the performance of the UKF with respect to the JS&PE task. The paper is structured as follows: Sec. 2 defines the problem statement. Sec. 3 overviews the components of the proposed methodology. Section 4 describes the application study, while in Sec. 5 directions for further research along this direction are outlined.

## 2. Problem Statement

Assume a nonlinear structure, which is actively controlled, per the setting illustrated in Fig. 1. The system described by the following nonlinear equation of motion:

$$\mathbf{M}\ddot{\mathbf{x}}(t) + \mathbf{r}(\mathbf{x}(t), \dot{\mathbf{x}}(t), \theta) = \mathbf{P}_d(\theta)\mathbf{u}_d(t) + \mathbf{P}_c(\theta)\mathbf{u}_c(t) \quad (1)$$

where  $\mathbf{x}, \dot{\mathbf{x}}, \ddot{\mathbf{x}} \in \mathbb{R}^n$  denotes the displacement vector and its derivatives; the velocity and acceleration respectively  $\mathbf{r}$  denotes the nonlinear restoring force, which forms a function of the displacement and velocity vectors, as well as the parameter vector  $\theta \in \mathbb{R}^p$ . The latter describes the vector of system parameters and may include parameters, which define a linear dependence, e.g. viscous damping, as well as coefficients of nonlinear terms, e.g. cubic or hysteretic nonlinearities.  $\mathbf{M} \in \mathbb{R}^{n \times n}$  denotes the mass matrix, and  $\mathbf{u} = [\mathbf{u}_d \quad \mathbf{u}_c]^T \in \mathbb{R}^{n_d+n_c}$  defines the combined input vector, which comprises an external disturbance term  $\mathbf{u}_d$  and the applied control force vector  $\mathbf{u}_c$ , with the selection vectors  $\mathbf{P}_d, \mathbf{P}_c$  further defining the degrees of freedom these forces are applied to.

The former nonlinear dynamics eq. (1) may be brought into a nonlinear state-space form, via introduction of the state vector  $\xi = [\mathbf{x} \quad \dot{\mathbf{x}}] \in \mathbb{R}^{2n}$

$$\begin{aligned} \dot{\xi} &= \begin{bmatrix} \dot{\mathbf{x}} \\ \dot{\dot{\mathbf{x}}} \end{bmatrix} = \begin{bmatrix} \dot{\mathbf{x}} \\ -\mathbf{M}^{-1}\mathbf{r}(\mathbf{x}(t), \dot{\mathbf{x}}(t), \theta) \end{bmatrix} + \begin{bmatrix} 0 \\ \mathbf{M}^{-1}\mathbf{P}_d(\theta)\mathbf{u}_d(t) + \mathbf{M}^{-1}\mathbf{P}_c(\theta)\mathbf{u}_c(t) \end{bmatrix} \Rightarrow \\ \dot{\xi} &= f_c(\xi, \mathbf{u}, \theta) \end{aligned} \quad (2)$$

$f_c$  is the nonlinear function defining the process equation, expressed in the continuous time domain. It will later be shown that the control force is chosen so as to cancel the nonlinear portion of the state equation, resulting in a nonlinear function of the dynamic states and parameter vector:  $\mathbf{u}_c(\xi, \theta) = -\mathcal{N}^*(\xi, \theta)$ .



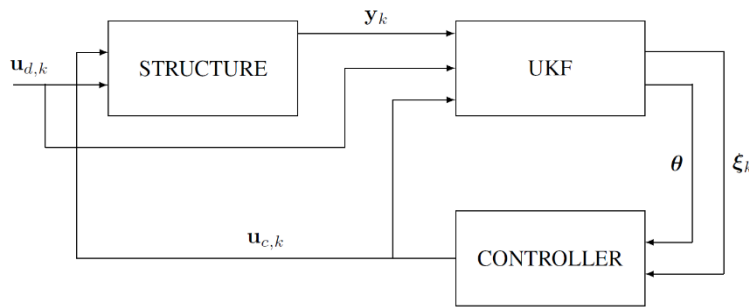


**Fig. 1.** Layout of the proposed nonlinear vibration control scheme.

The system is assumed to be monitored, with measurements of response quantities delivered in the form of displacement, velocities or accelerations, aggregated in the vector  $\mathbf{y} \in \mathbb{R}^m$ , defined, in turn, as a nonlinear function  $h_c$  of the dynamic state vector  $\xi$ , the driving input forces summarized in  $\mathbf{u}$ , and the parameter vector  $\theta$ :

$$\mathbf{y} = h_c(\mathbf{x}(t), \dot{\mathbf{x}}(t), \theta) = h_c(\xi, \mathbf{u}, \theta) \quad (3)$$

The previous set of process and observation equations is expressed in the continuous domain. However, we assume that a discretization scheme can be adopted for bringing these equations into a discretized form. In this work, we opt for a simple forward Euler (explicit) scheme, which proves sufficient for the implementation of the system identification and control schemes. This yields the following set of equations in the discrete time domain

$$\begin{aligned} \xi_{k+1} &= f_d(\xi_k, \mathbf{u}_k, \theta_k) \\ \mathbf{y}_k &= h_c(\xi_k, \mathbf{u}_k, \theta_k) \end{aligned} \quad (4)$$

where  $k$  denotes the current time step and  $f_d$  denotes the discretized nonlinear state-space equation.

### 3. Method

#### 3.1 The Unscented Kalman Filter for Joint State & Parameter Estimation (JS&PE)

The assumption that the model description (state-space equation) and the observations that are extracted from the system (measurements) are inherently characterized by uncertainty. To achieve estimation of the underlying states in the face of these uncertainties, it is necessary to explicit account for these in the problem statement. To this end, a Bayesian filtering approach is adopted, whereby the previous set of equations is expanded to account for the so-called process and measurement noise sources  $\mathbf{w}_k, \mathbf{v}_k$  respectively:

$$\begin{aligned} \xi_{k+1} &= f_d(\xi_k, \mathbf{u}_k, \theta_k) + \mathbf{w}_k \\ \mathbf{y}_k &= h_c(\xi_k, \mathbf{u}_k, \theta_k) + \mathbf{v}_k \end{aligned} \quad (5)$$

Both noise sources are assumed to be normally distributed as  $\mathbf{w}_k \sim N(\mathbf{0}, \mathbf{Q})$ , and  $\mathbf{v}_k \sim N(\mathbf{0}, \mathbf{R})$ , with  $\mathbf{Q} \in \mathbb{R}^{2n \times 2n}, \mathbf{R} \in \mathbb{R}^{m \times m}$ , denoting the associated covariance matrices. The process noise serves for representing uncertainties that affect the governing equation of the dynamic system (state equation). These stem from model discrepancy, and additionally could reflect uncertainties in the input driving the system, whose measurement is often corrupt with noise. The measurement noise on the other hand reflects the uncertainty in the observation equation, and may again be linked to modeling discrepancies, and noise corruption of the feedforward term, as well as noise corrupting the observation itself (due to limited sensor precision, etc). Our specific estimation goal here lies in inference of both the unknown dynamic states  $\xi_k$ , which are not directly observed, as well as the unknown system parameters that have been aggregated in vector  $\theta_k$ . This is feasible in the context of the previously outline framework, via simple augmentation of the dynamic state vector  $\xi_k$  into the augmented vector  $\bar{\xi}_k = [\xi_k \ \theta_k]^T$ , which has been expanded to include the parameter vector  $\theta_k$ . In doing so, the evolution of the parameters must be defined. To this end, a fictitious random-walk equation for the unknown parameter vector is introduced as

$$\theta_{k+1} = \theta_k + \mathbf{w}_{\theta,k} \quad (6)$$

where  $\mathbf{w}_{\theta,k}$  is a zero mean Gaussian process noise of covariance matrix  $\Theta \in \mathbb{R}^{p \times p}$ . The zero mean Gaussian process noise  $\mathbf{w}_k$  of covariance matrix  $\mathbf{Q}$  is assumed uncorrelated with  $\mathbf{w}_{\theta,k}$ . The augmented nonlinear equations then become:

$$\begin{aligned} \bar{\xi}_{k+1} &= f(\bar{\xi}_k, \mathbf{u}_k) + \mathbf{w}_{a,k} \\ \mathbf{y}_k &= h(\bar{\xi}_k, \mathbf{u}_k) + \mathbf{v}_k \end{aligned} \quad (7)$$

$f, h$  now denote the augmented set of functions which account for inclusion of the parameters  $\theta_k$  in the augmented state vector  $\bar{\xi}_k$ . As a result of the uncorrelatedness between  $\mathbf{Q}, \Theta$ , the augmented process noise  $\mathbf{w}_{a,k}$  also results as zero mean with a covariance matrix that is expressed as  $\mathbf{Q}_a = \text{diag}\{\mathbf{Q}, \Theta\}$

Due to the nonlinear form of the state-space equations the adoption of a nonlinear Bayesian filter is proposed herein for the purpose of joint state and parameter estimation, namely, the Unscented Kalman Filter (UKF). The Unscented Kalman filter is chosen herein in place of simpler formulations, as for example the Extended Kalman Filter (EKF) [5],[50], since it has proven more adept in the handling of higher order nonlinearities and noise contamination [51].



**Table 1.** The general scheme of the UKF algorithm for joint state and parameter estimation.

<p>1. Further augment the state vector, further including the noise parameters  <math>\hat{\xi}_{k-1}^a = [\bar{\xi}_{k-1}^T, \mathbf{w}_{a,k-1}^T, \mathbf{v}_{k-1}^T]^T</math></p> <p><b>Initialization - <math>t_0</math></b></p> $\hat{\xi}_0 = \mathbb{E}[\bar{\xi}_0], \mathbf{P}_0 = \mathbb{E}\left[(\bar{\xi}_0 - \hat{\xi}_0)(\bar{\xi}_0 - \hat{\xi}_0)^T\right]$ $\hat{\xi}_0^a = \mathbb{E}[\bar{\xi}_0^a] = [\hat{\xi}_0^T \ 0 \ 0]^T, \mathbf{P}_0^a = \mathbb{E}\left[(\bar{\xi}_0^a - \hat{\xi}_0^a)(\bar{\xi}_0^a - \hat{\xi}_0^a)^T\right] = \begin{bmatrix} \mathbf{P}_0 & \mathbf{0} & \mathbf{0} \\ \mathbf{0} & \mathbf{Q}_a & \mathbf{0} \\ \mathbf{0} & \mathbf{0} & \mathbf{R} \end{bmatrix}$ <p><b>Time increment - <math>t_k</math></b>  <u>The Unscented Transform (UT)</u></p> <p>2. Formulation of the Sigma Point vector:  where <math>\alpha, \lambda</math> are parameters of the UT [20]; <math>L</math> is the dimension of the augmented state vector <math>\bar{\xi}_{k-1}^a</math></p> <p><b>Prediction stage:</b></p> <p>3. Propagation of the Sigma points through the system model, where dependence on the input term <math>\mathbf{u}</math> is removed for simplicity:  <math>\mathcal{X}_{k k-1}^{\xi,i} = f(\mathcal{X}_{k-1}^{\xi,i}, \mathcal{X}_{k-1}^{w,i}), i = 0,..,2L</math></p> <p>4. Calculation of the state and covariance priors:  <math>\hat{\xi}_{k k-1} = \sum_{i=0}^{2L} w_i^{\xi} \mathcal{X}_{k k-1}^{\xi,i}; \quad \mathbf{P}_{k k-1} = \sum_{i=0}^{2L} w_i^p [\mathcal{X}_{k k-1}^{\xi,i} - \hat{\xi}_{k k-1}] [\mathcal{X}_{k k-1}^{\xi,i} - \hat{\xi}_{k k-1}]^T</math>  with the sigma point weights <math>w_i^{\xi}, w_i^p</math> defined as in [20].</p> <p><b>Update stage:</b></p> <p>5. Calculation of Kalman gain:  <math>\mathbf{K}_k = \mathbf{P}_k^{\xi y} (\mathbf{P}_k^{yy})^{-1}</math>, where  <math>\mathbf{P}_k^{yy} = \sum_{i=0}^{2L} w_i^p [h(\mathcal{X}_{k k-1}^{\xi,i}) - \hat{\mathbf{y}}_{k k-1}] [h(\mathcal{X}_{k k-1}^{\xi,i}) - \hat{\mathbf{y}}_{k k-1}]^T, \quad \mathbf{P}_k^{\xi y} = \sum_{i=0}^{2L} w_i^p [\mathcal{X}_{k k-1}^{\xi,i} - \hat{\xi}_{k k-1}] [h(\mathcal{X}_{k k-1}^{\xi,i}) - \hat{\mathbf{y}}_{k k-1}]^T</math></p> <p>6. Improve the predictions of the state (posterior estimates) using the latest observations:  <math>\hat{\mathbf{y}}_{k k-1} = \sum_{i=0}^{2L} w_i^p h(\mathcal{X}_{k k-1}^{\xi,i}, \mathcal{X}_{k-1}^{w,i})</math>  <math>\hat{\xi}_k = \hat{\xi}_{k k-1} + \mathbf{K}_k (\mathbf{y}_k - \hat{\mathbf{y}}_{k k-1})</math>  <math>\mathbf{P}_k = \mathbf{P}_{k k-1} - \mathbf{K}_k \mathbf{P}_k^{yy} \mathbf{K}_k^T</math></p>
--

The UKF functions by modeling the state as a Gaussian random variable whose distribution can be approximated by a structured set of sample points; the sigma points. By means of the Unscented Transform (UT) [20], the sigma points capture the prior mean and covariance of the state and when propagated through the nonlinear function, provide an improved posterior estimate of the transformed state. For reasons of completeness, the steps of the UKF are briefly summarized in Table 1, however the interested reader is pointed to [52],[53] for a more elaborate description of the UKF formulation for joint state and parameter identification in nonlinear systems.

### 3.2 State-Feedback Linearization

The basic idea of linearization using feedback is described in [54]. The main idea is to design the feedback control signal, so as to linearize the state equation, i.e., effectively cancel out the nonlinear term. In order to elaborate on this procedure we split the general nonlinear state function  $f_c(\xi, \mathbf{u}, \theta)$  from equation (2) into four components, as follows:

$$\dot{\xi} = f_c(\xi, \mathbf{u}, \theta) \Rightarrow \dot{\xi} = \mathbf{A}(\theta)\xi + \mathcal{N}(\xi, \theta) + \mathbf{B}_d(\theta)\mathbf{u}_d + \mathbf{B}_c(\theta)\mathbf{u}_c \quad (8)$$

The above equation splits the nonlinear state equation into four individual contributions, namely a term expressing linear dependence on the state  $\mathbf{A}(\theta)\xi$ , a term expressing nonlinear dependence on the state  $\mathcal{N}(\xi, \theta)$ , and the two terms  $\mathbf{B}_d\mathbf{u}_d, \mathbf{B}_c\mathbf{u}_c$  expressing dependence on the disturbance and control force, respectively. The input matrices  $\mathbf{B}_d, \mathbf{B}_c$  are associated to the input matrices of the original dynamic equation (eq.(1)) in the displacement space  $\mathbf{x}$  as  $\mathbf{B}_d = [\mathbf{0} \ \mathbf{P}_d]^T, \mathbf{B}_c = [\mathbf{0} \ \mathbf{P}_c]^T$ , with dependence on the parameter vector  $\theta$  omitted for simplicity. Following the elaboration offered by Wagg and Neild [54], for the general case,  $\mathcal{N}(\xi, \theta)$  can be rewritten as  $\mathcal{N}(\xi, \theta) = \mathbf{B}_c(\theta)\mathcal{N}^*(\xi, \theta)$ , thus leading to the following formulation:

$$\begin{aligned} \dot{\xi} &= f_c(\xi, \mathbf{u}, \theta) \Rightarrow \dot{\xi} = \mathbf{A}(\theta)\xi + \mathbf{B}_c(\theta)\mathcal{N}^*(\xi, \theta) + \mathbf{B}_d(\theta)\mathbf{u}_d + \mathbf{B}_c(\theta)\mathbf{u}_c \\ \dot{\xi} &= \mathbf{A}(\theta)\xi + \mathbf{B}_d(\theta)\mathbf{u}_d + \mathbf{B}_c(\theta)(\mathcal{N}^*(\xi, \theta) + \mathbf{u}_c) \end{aligned} \quad (9)$$

Setting  $\mathbf{u}_{c,NL} = -\mathcal{N}^*(\xi, \theta)$  linearizes the nonlinear state equation, and therefore determines the desired feedback linearization control signal for the system. It is assumed that the system states in the expression  $\mathcal{N}^*$  can be readily accessed for use in the



control signal  $\mathbf{u}_{c,NL}$ . Nonlinear dynamical systems, which can be expressed in the form of equation (9) can be linearized using the feedback control signal. This formulation comprises a subset of the more general form, which was utilized for elaboration of the joint state and parameter identification framework. This implies that the JS&PE scheme continues to apply, per the definition offered in section 3.1. The control signal may include additional control tasks, such as the addition of damping. Beyond its functionality for cancellation of the nonlinear terms, the general control input is chosen as  $\mathbf{u}_c = \mathbf{u}_{c,NL} + \mathbf{u}_{c,L} = -\mathcal{N}^*(\xi, \theta) + c(\cdot)$ , where  $c(\cdot)$  is the desired control function, e.g. the compensation required for vibration mitigation. If the underlying linear system is inherently unstable, then the control function should be chosen so as to ensure a stable linear control after cancellation of the nonlinear terms.

In what we propose herein, an adaptive framework is followed since  $\mathbf{u}_{c,NL}(\xi, \theta) = -\mathcal{N}^*(\xi, \theta)$  also depends on system parameters  $\theta$ , which are estimated via the JS&PE scheme, i.e., via use of the UKF. An alternative to this approach would be the adaptive scheme proposed by Wagg and Neild in [54] (§3.7.1), where a set of time varying control gains is inserted in the expression of  $\mathbf{u}_c$ . In contrast to the latter approach, the UKF based scheme we propose separates the estimation step of the uncertain parameters from the calculation of the adaptive control gain. The latter is succeeded via an LQR approach, where the gain is calculated using only the linear portion of the state equation  $\mathbf{A}(\theta)\xi$ , upon removal of the nonlinear term via state-feedback linearization.

### 3.3 Linear-Quadratic Regulator (LQR)

We describe adoption of the LQR on the linear system obtained via feedback linearization, which comprises the following state-space form (in discrete-time):

$$\begin{aligned}\xi_{k+1} &= \bar{\mathbf{A}}(\theta)\xi_k + \bar{\mathbf{B}}_d(\theta)\mathbf{u}_{d,k} + \bar{\mathbf{B}}_c(\theta)\mathbf{u}_{c,L,k} \\ \mathbf{y}_k &= \mathbf{C}(\theta)\xi_k + \mathbf{D}(\theta)\mathbf{u}_{c,L,k} + \mathbf{NL}(\cdot)\end{aligned}\quad (10)$$

where  $\bar{\mathbf{A}}(\theta), \bar{\mathbf{B}}_c(\theta), \bar{\mathbf{B}}_d(\theta)$  are the discretized state and input matrices, obtained via use of a zero-order hold scheme applied on the continuous matrices  $\mathbf{A}(\theta), \mathbf{B}_c(\theta), \mathbf{B}_d(\theta)$  of eq. (8),  $\mathbf{u}_d$  is the disturbance vector,  $\mathbf{u}_{c,L}$  is the linearized control force, i.e., the component of the force that is applied additionally to the term  $\mathbf{u}_{c,NL}$ , which served for cancellation of the nonlinear state components, and  $k = 1, 2, 3, \dots, T$  are the time discrete time steps. In order to proceed with implementation of the LQR scheme, the observation function  $h_c(\xi_k, \mathbf{u}_k, \theta_k)$  is segregated into a linear  $\mathbf{C}(\theta)\xi_k + \mathbf{C}(\theta)\mathbf{u}_{c,L,k}$  and nonlinear (remainder) part  $\mathbf{NL}(\cdot)$ .

The LQR control scheme is established on the principle of minimizing the following cost function  $J$

$$J = \sum_{k=0}^{\infty} (\xi_k^T \mathbf{Q}_{LQR} \xi_k + \mathbf{u}_{c,L,k}^T \mathbf{R}_{LQR} \mathbf{u}_{c,L,k} + 2\xi_k^T \mathbf{N}_{LQR} \mathbf{u}_{c,L,k}) \quad (11)$$

where,  $\mathbf{Q}_{LQR}, \mathbf{R}_{LQR}, \mathbf{N}_{LQR}$  designate positive definite weighting parameters [55],[56]. From Lublin and Athans [57] (Theorem 17.2), it can be shown that

$$\begin{aligned}\mathbf{Q} &= \mathbf{C}^T(\theta)\mathbf{C}(\theta), \\ \mathbf{R} &= \mathcal{R} + \mathbf{D}^T(\theta)\mathbf{D}(\theta) \text{ and} \\ \mathbf{N} &= \mathbf{C}^T(\theta)\mathbf{D}(\theta)\end{aligned}\quad (12)$$

where  $\mathcal{R}$  is a free selection matrix. The optimal control force vector is estimated by adopting

$$\mathbf{u}_{c,L,k} = -\mathbf{K}(\theta)\xi_k \quad (13)$$

$\mathbf{K}(\theta)$  is the optimal feedback gain, which minimizes the cost function  $J$ , and is obtained via the equation  $(\bar{\mathbf{B}}_c^T \bar{\mathbf{S}} \bar{\mathbf{B}}_c + \mathbf{R}_{LQR})\mathbf{K} = \bar{\mathbf{B}}_c^T \bar{\mathbf{S}} \bar{\mathbf{A}} + \mathbf{N}_{LQR}^T$ . The optimality condition for the LQR heavily relies on the selection of the weight factors  $\mathbf{Q}_{LQR}, \mathbf{R}_{LQR}, \mathbf{N}_{LQR}$ , which define the value of the variable  $\mathbf{S}$  via solution of the discrete time algebraic Riccati equation (DARE), where dependence on  $\theta$  is omitted for simplicity.

$$\mathbf{S} = \bar{\mathbf{A}}^T \bar{\mathbf{S}} \bar{\mathbf{A}} + (\bar{\mathbf{A}}^T \bar{\mathbf{S}} \bar{\mathbf{B}}_c + \mathbf{N}_{LQR})(\bar{\mathbf{B}}_c^T \bar{\mathbf{S}} \bar{\mathbf{B}}_c + \mathbf{R}_{LQR})^{-1} (\bar{\mathbf{B}}_c^T \bar{\mathbf{S}} \bar{\mathbf{A}} + \mathbf{N}_{LQR}^T) + \mathbf{Q}_{LQR} \quad (14)$$

For further information on the linear quadratic regulator the interested reader is referred to [55]. In case the liner matrices do not form a function of the parameter vector  $\theta$ , the Riccati equation is solved only once in the beginning of the computation. In case of dependence of these matrices on  $\theta$  an online, recursive implementation of eq. (14), based on the current value of  $\theta$ , is provided in [47].

## 4. Case Studies

### 4.1 The Duffing oscillator

For assessing the efficacy of the proposed method, the Duffing oscillator is first considered. The equation of motion reads

$$\ddot{x}(t) + \delta \dot{x}(t) + \beta x(t) + \alpha x^3(t) = u_d(t) + u_c(t) \quad (15)$$

where  $\alpha, \beta$  and  $\delta$  are parameters that control the nonlinear stiffness, the linear stiffness and the damping ratio, respectively, and  $u_d(t)$  and  $u_c(t)$  are the disturbance excitation and control force, respectively. Under harmonic disturbance, eq. (15) offers a very broad vibrating behavior, ranging from non-harmonic periodic to purely chaotic, depending on the amplitude of the excitation. In the following,  $\alpha$  is assumed as the uncertain parameter, while the rest admit the values listed in RRRR, adopted from [54] (see example 2.6). Notice that the model is characterized by negative linear stiffness.



**Table 2.** Parameters used for the simulation and control of the Duffing oscillator.

Parameter	Symbol	Values	Unit
Linear Stiffness	$\beta$	-1.000	N/m
Nonlinear stiffness (nominal)	$\alpha$	+1.000	N/m <sup>3</sup>
Damping	$\delta$	+0.400	Ns/m
Sampling period	$T_s$	1/4096	s
Simulation time	$T_{end}$	60	s
Augmented state-space: process noise covariance matrix	$\mathbf{Q}_a$	$10^{-8} \mathbf{I}_3$	-
Augmented state-space: measurement noise variance	$\sigma_{vv}^2$	$10^{-10}$	-
Augmented state vector: initial mean	$\hat{\xi}_0$	[0 0 0.8 $\alpha$ ]	-
Augmented state vector: initial covariance matrix	$\mathbf{P}_0$	$10^{-8} \mathbf{I}_3$	-
LQR controller parameter	$R$	1	-

Simulations are conducted by numerical integration of eq. (15) via a 4<sup>th</sup>-order Range-Kutta scheme, at a fixed sampling period and for 60s. The availability of noise-corrupted vibration acceleration response at 2% noise-to-signal ratio is assumed. The numerical values of all the parameters associated to the UKF and LQR tasks are also provided in RRRRR and kept unaltered for all the cases considered below, unless otherwise specified. Regarding the UKF, the augmented discrete-time state and output variables are calculated by

$$\begin{aligned}\xi_{1,k+1} &= \xi_{1,k} + T_s \xi_{2,k} \\ \xi_{2,k+1} &= \xi_{2,k} + T_s (-\delta \xi_{2,k} - \beta \xi_{1,k} - \xi_{3,k} \xi_{1,k}^3) + T_s u_{d,k} + T_s u_{c,k} \\ \xi_{3,k+1} &= \xi_{3,k}\end{aligned}\quad (16)$$

$$y_k = -\delta \xi_{2,k} - \beta \xi_{1,k} - \xi_{3,k} \xi_{1,k}^3 + u_{d,k} + u_{c,k} \quad (17)$$

where  $u_{c,k}$  is the control force

$$u_{c,k} = -\mathbf{K}_k \begin{pmatrix} \xi_{1,k} \\ \xi_{2,k} \end{pmatrix} + \xi_{3,k} \xi_{1,k}^3 \quad (18)$$

and  $\mathbf{K}_k$  the LQR control gain. In comparing the performance of the UKF, the EKF is also tested as an alternative Bayesian filter, using the same parameters listed in **Error! Reference source not found..**

Figures 2-5 present the results for a harmonic disturbance of the form

$$u_d(t) = \gamma \sin(2\pi ft) \quad (19)$$

with  $\gamma = 0.6$  and  $f = 0.286$  Hz. At this amplitude, the motion is non-harmonic periodic [54], with a non-zero-mean steady-state response. This is depicted in Fig. 2, left plot, where the uncontrolled displacement is displayed in black. The proposed method exhibits a quite satisfying performance, succeeding at both linearizing the uncertain equation of motion and suppressing the vibration levels due to the harmonic disturbance. This is apparent not only in the time-series of Fig. 2, but also in the phase planes of Fig. 3, where a clear shift to linearity is observed after the transient effects, at around half the vibration levels, compared to the uncontrolled system. At this excitation level, the UKF and the EKF produce identical results.

The behavior of the filters is, though, quite different regarding the estimation of the uncertain parameter. As indicated in Fig. 4, the UKF manages to keep the estimate of the uncertain parameter within a relative small range of the actual value, whereas the EKF-based estimate is characterized by a strong “oscillating” performance, with a mean value that is around 2, e.g. 100% over the actual value. Despite this inconsistency, the linearization and disturbance attenuation tasks are as good as the ones of the UKF. This is justified by plotting the restoring force, defined as

$$F(t) = -\beta x(t) - \alpha x^3(t) \quad (20)$$

In the uncontrolled case, Fig. 5 left, it is observed that at the resulted range of uncontrolled displacements the restoring force is rather linear and thus the nonlinear term has small effects on the measured vibration acceleration response, rendering the identification of  $\alpha$  a difficult task. The perfect linearity of the restoring force is confirmed in the middle (UKF) and right (EKF) plots of Fig. 5.

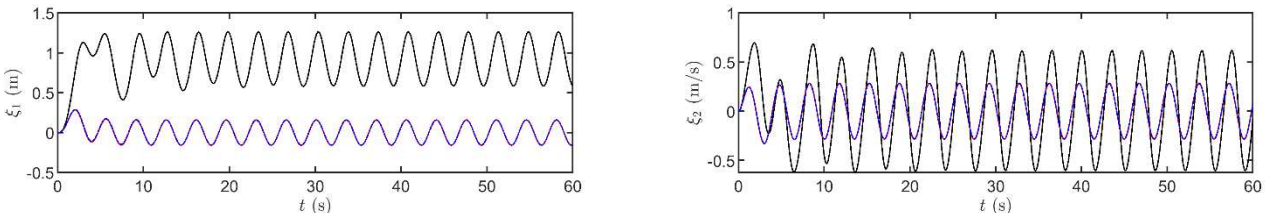


**Fig. 2.** Uncontrolled (in black) and controlled (UKF in red, EKF in blue) states for a harmonic disturbance with  $\gamma = 0.6$  and  $f = 0.286$  Hz. Left: displacement. Right: velocity (Duffing oscillator).



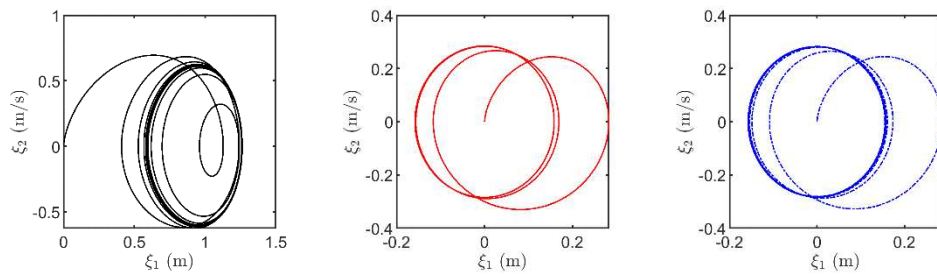


**Fig. 3.** Uncontrolled (left, in black) and controlled (middle: UKF, in red, right: EKF, in blue) phase plane for a harmonic disturbance with  $\gamma = 0.6$  and  $f = 0.286$  Hz (Duffing oscillator).

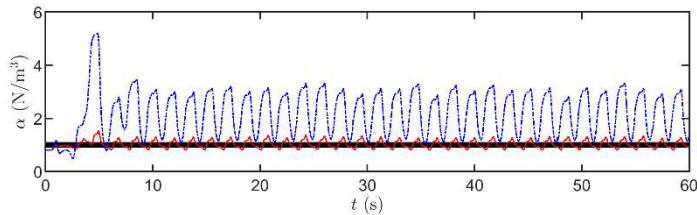


**Fig. 4.** Nominal (in black) and estimated (UKF in red, EKF in blue) parameter  $\alpha$  for a harmonic disturbance with  $\gamma = 0.6$  and  $f = 0.286$  Hz. In this subcase, the variance of the uncertain parameter has been increased to  $10^{-3}$  instead of  $10^{-8}$ , as the latter led to extremely slow convergence (Duffing oscillator).

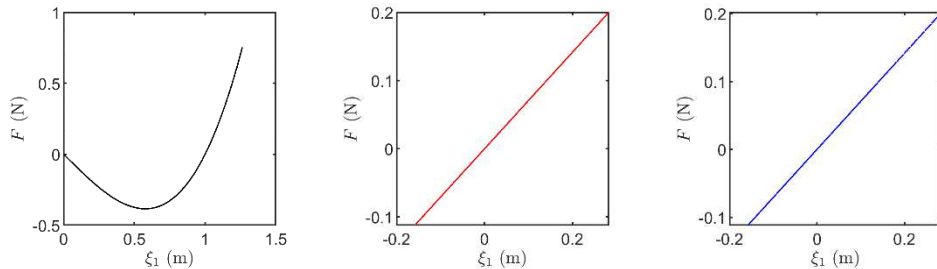


**Fig. 5.** Uncontrolled (left, in black) and controlled (middle: UKF, in red, right: EKF, in blue) restoring force for a harmonic disturbance with  $\gamma = 0.6$  and  $f = 0.286$  Hz (Duffing oscillator).

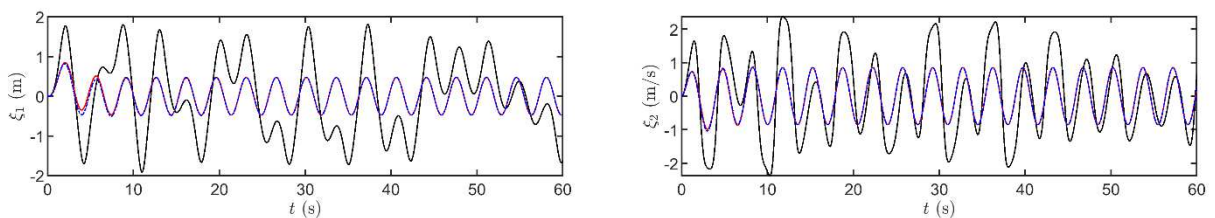


**Fig. 6.** Uncontrolled (in black) and controlled (UKF in red, EKF in blue) states for a harmonic disturbance with  $\gamma = 1.8$  and  $f = 0.286$  Hz. Left: displacement. Right: velocity (Duffing oscillator).

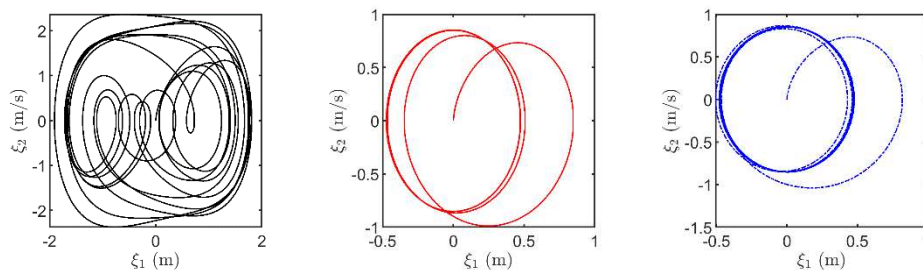


**Fig. 7.** Uncontrolled (left, in black) and controlled (middle: UKF, in red, right: EKF, in blue) phase plane for a harmonic disturbance with  $\gamma = 1.8$  and  $f = 0.286$  Hz.



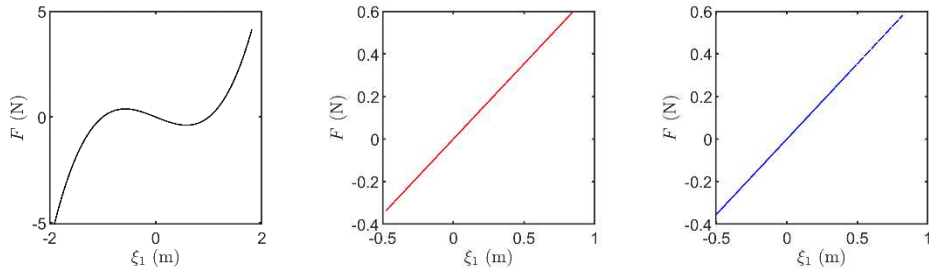


**Fig. 8.** Uncontrolled (left, in black) and controlled (middle: UKF, in red, right: EKF, in blue) restoring force for a harmonic disturbance with  $\gamma = 1.8$  and  $f = 0.286$  Hz (Duffing oscillator).

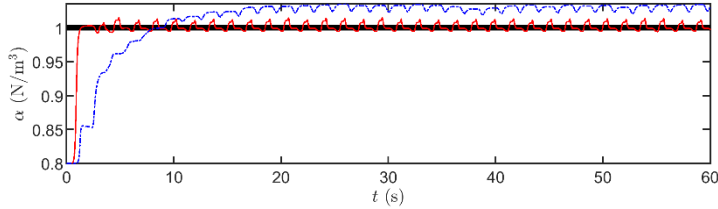


**Fig. 9.** Nominal (in black) and estimated (UKF in red, EKF in blue) parameter  $\alpha$  for a harmonic disturbance with  $\gamma = 1.8$  and  $f = 0.286$  Hz (Duffing oscillator).

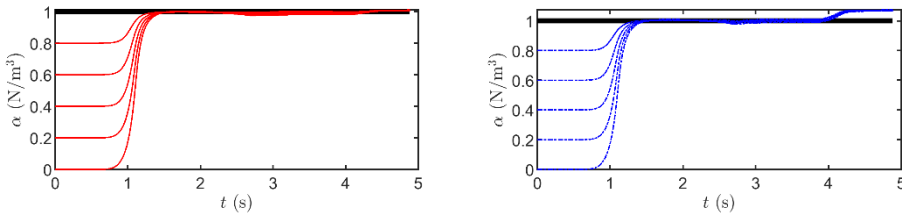


**Fig. 10.** Uncontrolled (left, in black) and controlled (middle: UKF, in red, right: EKF, in blue) phase plane for a harmonic disturbance with  $\gamma = 1.8$  and  $f = 0.286$  Hz (Duffing oscillator).

Increasing the amplitude to  $\gamma = 1.8$  causes a purely chaotic uncontrolled response, as shown in the time-series of Fig. 6 (in black) and the phase plane of Fig. 7 left. Again, the active controller has an excellent performance for both the UKF and the EKF, cancelling the nonlinearity and reducing the overall vibration levels from around  $\pm 2$  m to approximately  $\pm 0.5$  m (as indicated in the x-axis of the phase planes of Fig. 7, middle and right, for the UKF and the EKF, respectively). The result of the applied control is a zero-mean harmonic vibration displacement response in the steady-state (Fig. 6, left, in red and blue). Notice that at this excitation levels the uncontrolled restoring force exhibits a fully nonlinear behavior. This is depicted in Fig. 8, left, and allows for the correct estimation of the uncertain parameter. As Fig. 9 illustrates, the UKF again outperforms the EKF, both in terms of convergence rate and accuracy.

The nonlinear operating point of the system at this excitation levels further allows for an examination of the effects of the initial value for the uncertain parameter. In Fig. 10, the evolution of the estimate during the first 5s of the simulation is plotted, when the initial value is set at 0%, 20%, 40%, 60% and 80% of the true value. It is noted that for this set of simulations, the variance of the uncertain parameter has been increased to  $10^{-6}$ . The performance of both filters is quite similar, succeeding to quickly converge to the true value regardless the initial “guess”. The UKF, however, manages to maintain the converged value of the uncertain parameter after the occurrence of the transient effects (around the 4<sup>th</sup>s), in contrast to the EKF, which tends to destabilize.

In investigating the performance of the controller over a disturbance with much richer frequency content, Fig. 11-Fig. 14 display the results for a chirp signal with amplitude 1.8N and linear frequency increase from 0 to 2Hz. Within this band, the response of the uncontrolled oscillator contains several subharmonics and non-integer harmonics. In this case, the main contributions of the controller are (i) to bring the mean value of the steady-state displacement response to zero; and (ii) to reduce the overall transient vibration levels, both in displacement and velocity. The uncertain parameter is slightly overestimated from both the UKF and the EKF; this is shown in Fig. 13.

As a final note on the performance of the UKF and EKF, Table 3 displays the computational load of the filters during simulation, by measuring the total time required for code execution during each loop. The computational load is interpreted as mean value and variance and, expectedly, indicates that (i) the EKF requires slightly fewer recourses compared to the UKF; and (ii) the EKF appears as more “computationally consistent”, as its variance is one order of magnitude smaller than the one of the UKF. Still, the latter filter succeeds in performing calculations at one order of magnitude less than the sampling period ( $1/4096=2.4414 \times 10^{-4}$  s), implying thus no effects on the stability of the control loop, while it must be mentioned that no UKF code optimization was carried out.

#### 4.2 The Bouc-Wen model

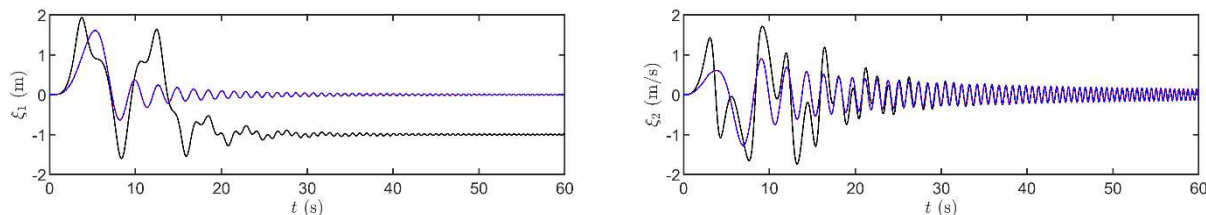
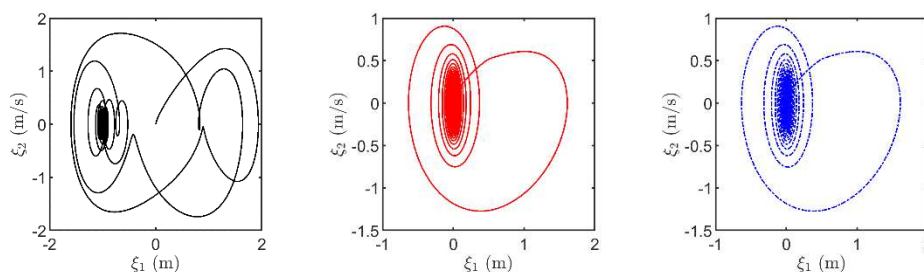
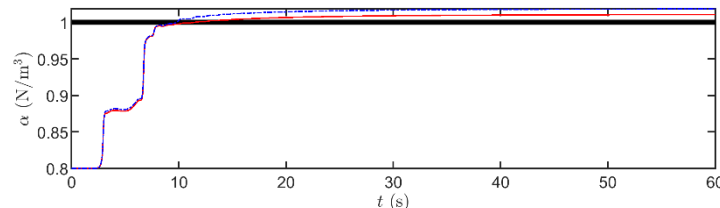
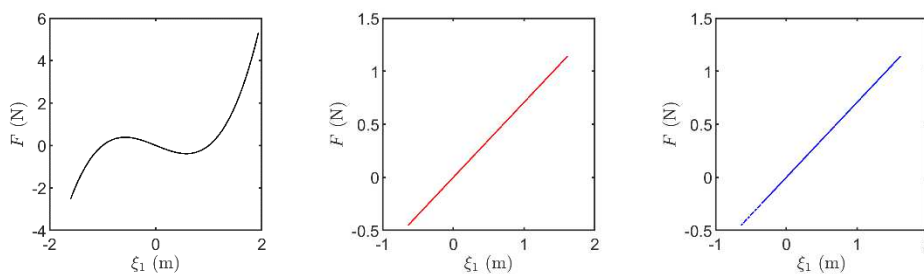
The second case study considered pertains to the Bouc-Wen model, which is described by the structural equation

$$m\ddot{x}(t) + c\dot{x}(t) + \alpha kx(t) + (1 - \alpha)kz(t) = u_d(t) + u_c(t) \quad (21)$$



**Table 3.** Mean elapsed time and associated variance for the execution of the UKF and EKF during each of the excitation cases of the Duffing oscillator.

Excitation	UKF		EKF	
	mean	variance	mean	variance
Sinusoidal ( $\gamma = 0.6$ and $f = 0.286$ Hz)	$4.91 \times 10^{-5}$	$4.41 \times 10^{-9}$	$4.44 \times 10^{-5}$	$1.27 \times 10^{-10}$
Sinusoidal ( $\gamma = 1.8$ and $f = 0.286$ Hz)	$5.05 \times 10^{-5}$	$1.77 \times 10^{-9}$	$4.48 \times 10^{-5}$	$1.92 \times 10^{-10}$
Chirp excitation	$5.06 \times 10^{-5}$	$3.19 \times 10^{-9}$	$4.50 \times 10^{-5}$	$1.84 \times 10^{-10}$

**Fig. 11.** Uncontrolled (in black) and controlled (UKF in red, EKF in blue) states for a chirp disturbance. Left: displacement. Right: velocity (Duffing oscillator).**Fig. 12.** Uncontrolled (left, in black) and controlled (middle: UKF, in red, right: EKF, in blue) phase plane for a chirp disturbance (Duffing oscillator).**Fig. 13.** Nominal (in black) and estimated (UKF in red, EKF in blue) parameter  $\alpha$  for a chirp disturbance (Duffing oscillator).**Fig. 14.** Uncontrolled (left, in black) and controlled (middle: UKF, in red, right: EKF, in blue) restoring force for a chirp disturbance (Duffing oscillator).

where, as previously,  $u_d(t)$  and  $u_c(t)$  are the disturbance excitation and control force, respectively,  $c$  and  $k$  correspond to viscous damping and linear stiffness, respectively,  $\alpha$  is the ratio of post-yield to pre-yield stiffness and  $z(t)$  is the hysteretic displacement that follows the equation

$$\ddot{z}(t) = \dot{x}(t) \left\{ A - [\beta \text{sign}(z(t)\dot{x}(t)) + \gamma] |z(t)|^n \right\} \quad (22)$$

in which  $A$ ,  $\beta$ ,  $\gamma$  and  $n$  are parameters that control the hysteretic behavior of the model and  $\text{sign}(\cdot)$  is the signum function. Simulations are conducted by numerical integration of eqs. (21)-(22) via a 4<sup>th</sup>-order Range-Kutta scheme, at a fixed sampling period and for 20s. It is assumed that  $\beta$  and  $\gamma$  are the uncertain parameters that must be estimated via the UKF. The augmented discrete-time state and output variables thus read



**Table 4.** Parameters used for the simulation and control of the Bouc-Wen model.

Parameter	Symbol	Values	Unit
Mass	$m$	65	N/m
Damping	$c$	150	Ns/m
Linear Stiffness	$k$	$4 \times 10^4$	N/m
Post-yield / pre-yield stiffness ratio	$\alpha$	$10^{-1}$	-
Bouc-Wen parameter A	$A$	1	-
Bouc-Wen parameter n	$n$	2	-
Sampling period	$T_s$	1/4096	s
Simulation time	$T_{end}$	20	s
Augmented state-space: process noise covariance matrix	$\mathbf{Q}_a$	$10^{-6} \mathbf{I}_5$	-
Augmented state-space: measurement noise variance	$\sigma_{vv}^2$	$10^{-10}$	-
Augmented state vector: initial mean	$\hat{\xi}_0$	[0 0 0 0 0] <sup>T</sup>	-
Augmented state vector: initial covariance matrix	$\mathbf{P}_0$	$10^{-8} \mathbf{I}_5$	-
LQR controller parameter	$R$	$10^{-12}$	-

$$\begin{aligned} \xi_{1,k+1} &= \xi_{1,k} + T_s \xi_{2,k} \\ \xi_{2,k+1} &= \xi_{2,k} + T_s \left( -\frac{c}{m} \xi_{2,k} - \frac{\alpha k}{m} \xi_{1,k} - \frac{(1-\alpha)k}{m} \xi_{3,k} \right) + \frac{T_s}{m} u_{d,k} + \frac{T_s}{m} u_{c,k} \\ \xi_{3,k+1} &= \xi_{3,k} + T_s \left( \xi_{2,k} \left( A - \left[ \xi_{4,k} \text{sign}(\xi_{2,k} \xi_{3,k}) \xi_{3,k} + \xi_{5,k} \right] \left| \xi_{3,k} \right|^n \right) \right) \\ \xi_{4,k+1} &= \xi_{4,k} \\ \xi_{5,k+1} &= \xi_{5,k} \end{aligned} \quad (23)$$

$$y_k = -\frac{c}{m} \xi_{2,k} - \frac{\alpha k}{m} \xi_{1,k} - \frac{(1-\alpha)k}{m} \xi_{3,k} + \frac{1}{m} u_{d,k} + \frac{1}{m} u_{c,k} \quad (24)$$

with eq. (24) corresponding to vibration acceleration data, corrupted at 2% noise-to-signal ratio. The control force is calculated by

$$u_{c,k} = -\mathbf{K}_k \begin{pmatrix} \xi_{1,k} \\ \xi_{2,k} \end{pmatrix} + (1-\alpha)k \xi_{3,k} \quad (25)$$

where  $\mathbf{K}_k$  is the LQR control gain, while the disturbance is again assumed periodic of the form

$$u_d(t) = 4000 \sin\left(\sqrt{\frac{k}{m}} t\right) \quad (26)$$

e.g. the excitation frequency equals the natural frequency of the linearized system. The numerical values of the involved parameters are listed in Table 4.

The performance of the method for the Bouc-Wen model is illustrated in Fig. 15-Fig. 18. It is noted that at this parameter space the EKF fails to converge, and thus no comparisons are presented. In contrast, the UKF performs quite efficiently. In specific, the method succeeds in cancelling the nonlinearity and reducing the overall vibration levels approximately 50% (as observed in the displacement time-series of Fig. 15 and the x-axes of the phase planes of Fig. 16), while the uncertain parameters are estimated with high accuracy and relative fast convergence. As in the Duffing oscillator, the nonlinear hysteretic restoring force in the uncontrolled model is replaced by a linear curve of sufficiently lower range and this can be confirmed by comparing the y-axes of Fig. 18. The mean elapsed time and its variance in this case is  $5.43 \times 10^{-5}$  s and  $5.35 \times 10^{-10}$ , respectively, confirming the potential of the UKF to be implemented as a real-time filter. An issue that deserves further attention is the range of the transient response of the controlled displacement (Fig. 15, left plot, red curve), which results amplified, indicating an "overshoot" before it reaches the steady-state. This is attributed to the transient second-order dynamics of the resulted controlled system and could be suppressed by placing a PID controller in parallel to the system.

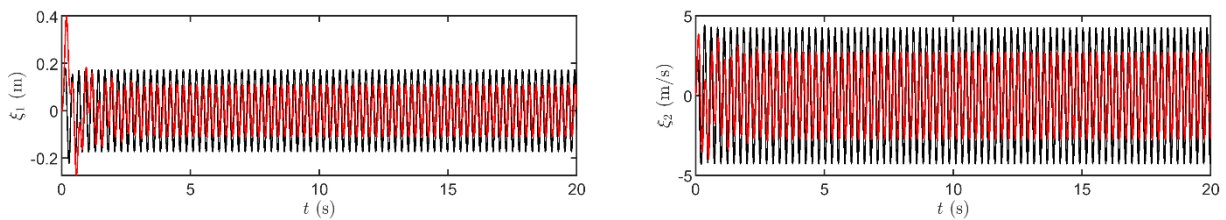


**Fig. 15.** Uncontrolled (in black) and controlled (in red) states for a harmonic disturbance. Left: displacement. Right: velocity (Bouc-Wen model).



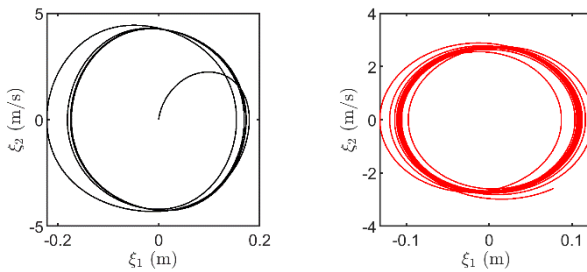


**Fig. 16.** Uncontrolled (left, in black) and controlled (right, in red) phase plane (Bouc-Wen model).

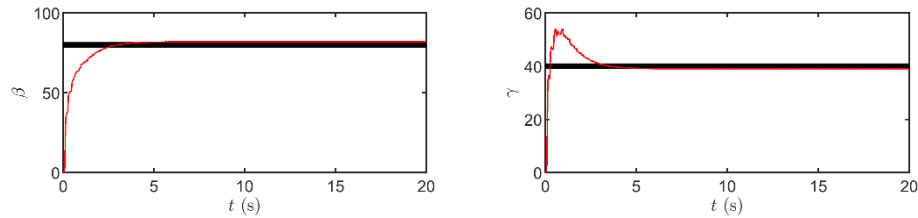


**Fig. 17.** Nominal (in black) and estimated (in red) parameters. Left:  $\beta$ , right:  $\gamma$  (Bouc-Wen model).

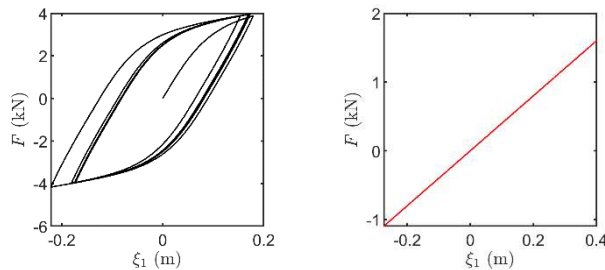


**Fig. 18.** Uncontrolled (left, in black) and controlled (right, in red) restoring force (Bouc-Wen model).

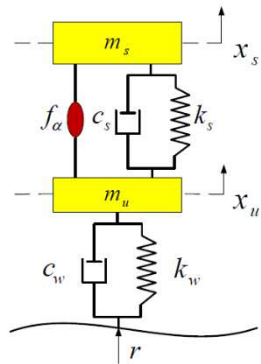


**Fig. 19.** Sketch of the quarter-car model of a passenger vehicle.

#### 4.3 The quarter-car vehicle

The final paradigm used for the assessment of the method corresponds to a quarter-car model of a passenger vehicle, shown in Fig. 19. The tire is modelled as an unsprung mass ( $m_u$ ) of equivalent stiffness ( $k_w$ ) and damping ( $c_w$ ) and it is connected to the chassis (sprung mass  $m_s$ ) through a nonlinear suspension. The equations of motion are

$$\begin{aligned} m_u \ddot{x}_u(t) &= -(k_w + k_s)x_u(t) + k_s x_s(t) - f_{nl}(t) + k_w r(t) + c_w \dot{r}(t) + f_a(t) \\ m_s \ddot{x}_s(t) &= k_s x_u(t) - k_s x_s(t) + f_{nl}(t) - f_a(t) \end{aligned} \quad (27)$$

where  $r(t)$  is the road surface profile,  $f_a(t)$  is the applied active control force and  $f_{nl}(t)$  is the nonlinear suspension force, given by

$$f_{nl}(t) = c_s \text{sign}(x_u(t) - x_s(t))(x_u(t) - x_s(t))^2 \quad (28)$$



**Table 5.** Parameters used for the simulation and control of the quarter-car model.

Parameter	Symbol	Values	Unit
Unsprung mass	$m_u$	38	kg
Sprung mass	$m_s$	238	kg
Tire stiffness	$k_w$	$135 \times 10^3$	N/m
Tire damping	$c_w$	0	Ns/m
Suspension stiffness	$k_s$	$157 \times 10^2$	N/m
Suspension damping	$c_s$	200	Ns <sup>2</sup> /m <sup>2</sup>
Sampling period	$T_s$	1/4096	s
Simulation time	$T_{end}$	30	s
Augmented state-space: process noise covariance matrix	$\mathbf{Q}_a$	$10^{-8} \mathbf{I}_5$	-
Augmented state-space: measurement noise variance	$\sigma_{vv}^2$	$10^{-10}$	-
Augmented state vector: initial mean	$\hat{\xi}_0$	[0 0 0 0 0] <sup>T</sup>	-
Augmented state vector: initial covariance matrix	$\mathbf{P}_0$	$10^{-8} \mathbf{I}_5$	-
LQR controller parameter	$\mathcal{R}$	$10^{-10}$	-

with  $c_s$  denoting a damping constant. Equation 27 describes a damper with a simple orifice allowing fluid flow, frequently met in practical applications, in which the nonlinear force arises as the result of dynamic energy dissipation in the fluid.

As in the previous case studies, simulations are conducted by numerical integration of eq. (27) via a 4<sup>th</sup>-order Range-Kutta scheme, at a fixed sampling period and for 30s, assuming the tire stiffness as the uncertain parameter and the chassis acceleration as the noise-corrupted measured output (2% noise-to-signal ratio). The augmented discrete-time state-space mode is formulated as

$$\begin{aligned} \xi_{1,k+1} &= \xi_{1,k} + T_s \xi_{2,k} \\ \xi_{2,k+1} &= \xi_{2,k} + T_s \xi_{4,k} \\ \xi_{3,k+1} &= \xi_{3,k} + T_s \left( -\frac{\xi_{5,k} + k_s}{m_u} \xi_{1,k} + \frac{k_s}{m_u} \xi_{2,k} - \frac{c_s}{m_u} \text{sign}(\xi_{3,k} - \xi_{4,k})(\xi_{3,k} - \xi_{4,k})^2 \right) + T_s \frac{\xi_{5,k}}{m_u} r_k + T_s \frac{1}{m_u} f_{a,k} \\ \xi_{4,k+1} &= \xi_{4,k} + T_s \left( \frac{k_s}{m_s} \xi_{1,k} - \frac{k_s}{m_s} \xi_{2,k} + \frac{c_s}{m_s} \text{sign}(\xi_{3,k} - \xi_{4,k})(\xi_{3,k} - \xi_{4,k})^2 \right) - T_s \frac{1}{m_s} f_{a,k} \\ \xi_{5,k+1} &= \xi_{5,k} \end{aligned} \quad (29)$$

$$y_k = \frac{k_s}{m_s} \xi_{1,k} - \frac{k_s}{m_s} \xi_{2,k} + \frac{c_s}{m_s} \text{sign}(\xi_{3,k} - \xi_{4,k})(\xi_{3,k} - \xi_{4,k})^2 - \frac{1}{m_s} f_{a,k} \quad (30)$$

for a control force

$$f_{a,k} = -\mathbf{K}_k \begin{pmatrix} \xi_{1,k} \\ \xi_{2,k} \\ \xi_{3,k} \\ \xi_{4,k} \end{pmatrix} + c_s \text{sign}(\xi_{3,k} - \xi_{4,k})(\xi_{3,k} - \xi_{4,k})^2 \quad (31)$$

where  $\mathbf{K}_k$  is the LQR control gain. The road surface profile is generated in accordance to the Draft-ISO formulation [58] and corresponds to the average-quality one dimensional time-series of Fig. 20. The numerical values of all other parameters are listed in Table 5.

The behavior of the proposed active control strategy is expanded over Fig. 21-Fig. 23. As in the case of Bouc-Wen model, the EKF fails to converge using the parameter values of Table 5. On the contrary, the objective of improving passenger comfort is satisfied. In more detail, the chassis vibration levels are significantly reduced, as shown in Fig. 21 (top/bottom right plots): in particular, the controlled velocity (state  $\xi_4$ ) indicates that the chassis vibration acceleration, which is intimately related to the passenger comfort, is negligible. Expectedly, the controlled displacement and velocity of the tire are not reduced in a consistent manner. This is merely attributed to the absence of tire damping ( $c_w = 0$ ).

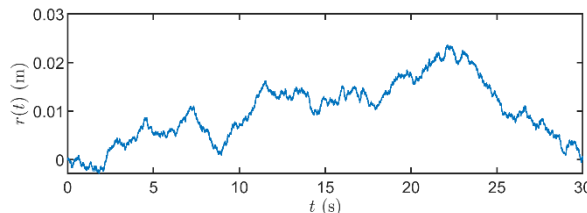


**Fig. 20.** The average-quality road profile applied as disturbance to the quarter-car control problem.



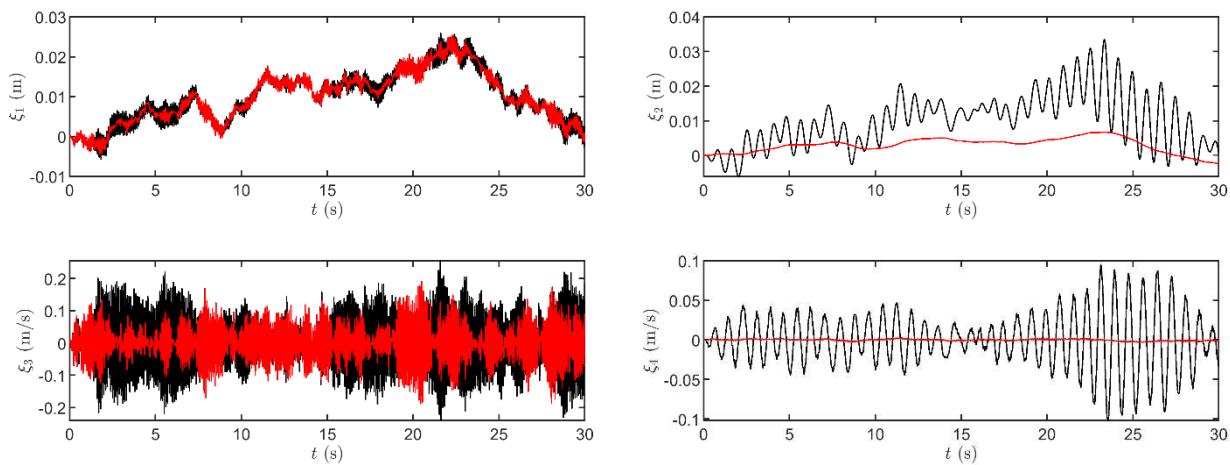


**Fig. 21.** Uncontrolled (in black) and controlled (in red) states for the road profile disturbance of Fig. 20. Top left: tire displacement. Top right: chassis displacement. Bottom left: tire velocity. Bottom right: chassis velocity (quarter-car model).

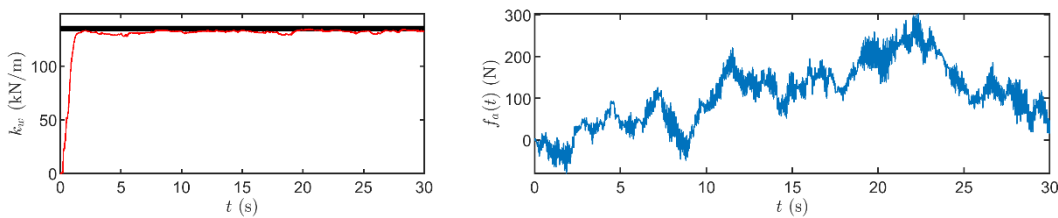


**Fig. 22.** Left: nominal (in black) and estimated (in red) tire stiffness. Right: evolution of the active control force of eq. (31) (quarter-car model).

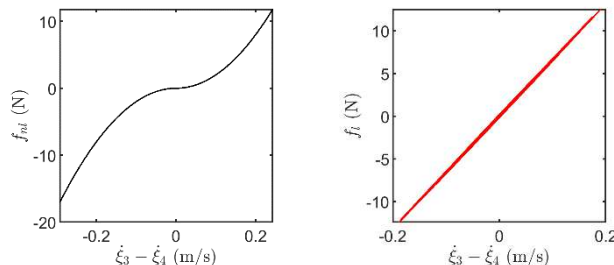


**Fig. 23.** Uncontrolled (left, in black) and controlled (right, in red) damping force vs. rattle space velocity (quarter-car model).

The estimation of the uncertain parameter (Fig. 22, left) is very accurate and is succeeded within the first 2s of the process, confirming the efficacy of the UKF, especially under stochastic disturbances with reach frequency content, as the one of Fig. 20. Notice that the time-series of the active control force (Fig. 22, right) follow the one of the road disturbance, and that the control amplitude levels are not very high, implying that the energy requirements are reasonable (indicatively the equivalent “weight” of the control force reaches approximately 30 kg, which is around the weight of the sprung mass). This result is closely related to the feedback linearization part (Fig. 23), which results in a linear damping force of lower range, compared to its nonlinear, uncontrolled counterpart. The computational cost of the active loop for this case study is  $4.81 \times 10^{-5}$ s and  $1.18 \times 10^{-9}$ , in terms of mean elapsed time and variance, respectively, again confirming the potential of the UKF to be implemented as a real-time filter.

## 5. Conclusion

We present a framework for the active control of nonlinear systems characterized by inherent uncertainties. Our method proceeds by isolating the nonlinear components and applying feedback linearization, under the assumption that the nonlinearities have well-defined mathematical expressions. The uncertain parameters are estimated via an augmented state-space model, while the associated nonlinear state estimation task is accomplished via the implementation of a nonlinear Bayesian estimator, namely the UKF. Accordingly, the active control force comprises two components: a first component ensuring removal of the nonlinear terms that are present in the state equation, and a second component implementing a typical LQR control law, for suppressing any external disturbance. The demonstrated results on the example case studies, across a broad range of nonlinear descriptions, suggest that the proposed Bayesian approach for nonlinear vibration control proves adept in the handling of uncertain systems.

The promising results of the proposed method introduce a path for further research. It would be interesting to compare the presented concept against other established, state-of-the art methods, such as the H-infinity, the model predictive and the three-stage controllers. This is a task, in which the authors are currently elaborating on. Moreover, the adopted assumption on the Gaussian nature of the process and measurement noise is an issue that should be further investigated. In this regard, previous work of the authoring team has shown that the UKF performs well, even for experimentally tested systems where this strict assumption may not hold [15],[59]. The unscented transform offers flexibility in this respect. Formulations for sigma points that are able to



capture the third moment (the skew) of an arbitrary distribution and the fourth moment (the kurtosis) of a symmetric distribution, shifting further away from the normal distribution assumption have also been developed [60]. In the event though where the noise distribution, and the resulting state statistics, shifts further away from Gaussianity, the more general Particle Filter, which is designed for this purpose ought to be used. These effects are elaborated upon in dedicated works of the authoring team [61], [62], [63], and do not pose a focus of this current work, where the normal distribution assumption is maintained for simplicity.

Finally, as the main aim of our study is to assess the feasibility of the proposed approach, a theoretical investigation on the stability, convergence, and robustness of the method is not developed. This remains an open issue that is currently considered by the authors, along with an experimental validation of the method.

## Author Contributions

V.K. Dertimanis initiated the project, developed the mathematical modelling, and conducted the numerical simulations; E.N. Chatzi and S.F. Masri examined and validated the mathematical modelling and assessed the numerical results. The manuscript was written through the contribution of all authors. All authors discussed the results, reviewed, and approved the final version of the manuscript.

## Conflict of Interest

The authors declare no potential conflicts of interest with respect to the research, authorship, and publication of this article.

## Funding

The second author would like to gratefully acknowledge support of this research by the Albert Lück Foundation.

## References

- [1] Basu, B., Bursi, O.S., Casciati, F., Casciati, S., Del Grosso, A.E., Domaneschi, M., Faravelli, L., Holnicki-Szulc, J., Irschik, H., Krommer, M., Lepidi, M., Martelli, A., Ozturk, B., Pozo, F., Pujol, G., Rakicevic, Z., Rodellar, J., A European Association for the Control of Structures Joint Perspective. Recent Studies in Civil Structural Control across Europe, *Structural Control and Health Monitoring*, 21(12), 2014, 1414–1436.
- [2] Lagaros, N., Plevris, V., Mitropoulou, C., Passive control systems for seismic damage mitigation, *Journal of Structural Engineering*, 124(5), 1998, 501–512.
- [3] Soong, T.T., Masri, S.F., Housner, G.W., An overview of active structural control under seismic loads, *Earthquake Spectra*, 7(3), 1991, 483–505.
- [4] Casciati, F., Magonette, G., Marazzi, F. (Eds), *Technology of Semiactive Devices and Applications in Vibration Mitigation*, John Wiley & Sons, Chichester, 2006.
- [5] Corigliano, A., Mariani, S., Parameter identification in explicit structural dynamics: performance of the extended Kalman filter, *Computer Methods in Applied Mechanics and Engineering*, 193(36–38), 2004, 3807–3835.
- [6] Egardt, B., *Stability of Adaptive Controllers*, Springer-Verlag, New York, USA, 1979.
- [7] Guclu, R., Yazici, H., Vibration control of a structure with ATMD against earthquake using fuzzy logic controllers, *Journal of Sound and Vibration*, 318(1–2), 2008, 36–49.
- [8] Ashour, O.N., Nayfeh, A.H., Adaptive Control of Flexible Structures Using a Nonlinear Vibration Absorber, *Nonlinear Dynamics*, 28, 2002, 309–322.
- [9] Casciati, F., Rodellar, J., Yildirim, U., Active and semi-active control of structures - theory and applications: A review of recent advances, *Journal of Intelligent Material Systems and Structures*, 23(11), 2012, 1181–1195.
- [10] Bitaraf M, Hurlebaus S., Semi-active adaptive control of seismically excited 20-story nonlinear building, *Engineering Structures*, 56, 2013, 2107–2118.
- [11] Weber, F., Robust force tracking control scheme for MR dampers, *Structural Control and Health Monitoring*, 22(12), 2015, 1373–1395.
- [12] Cetin S, Zergeroglu E, Sivrioglu S, Yuksek I., A new semiactive nonlinear adaptive controller for structures using MR damper: design and experimental validation, *Nonlinear Dynamics*, 66(4), 2011, 731–743.
- [13] Naets, F., Pastorino, R., Cuadrado, J., Desmet, W., Online state and input force estimation for multibody models employing extended Kalman filtering, *Multibody System Dynamics*, 32, 2014, 317–336.
- [14] Hoshiya, M., Saito, E., Structural Identification by Extended Kalman Filter, *Journal of Engineering Mechanics*, 110(12), 1984, 1757–1770.
- [15] Chatzi, E.N., Smyth, A.W., Masri, S.F., Experimental application of on-line parametric identification for nonlinear hysteretic systems with model uncertainty, *Journal of Structural Safety*, 32(5), 2010, 326–337.
- [16] Omrani, R., Hudson, R., Taciroglu, E., Parametric Identification of Nondegrading Hysteresis in a Laterally and Torsionally Coupled Building Using an Unscented Kalman Filter, *Journal of Engineering Mechanics*, 139(4), 2013, 452–468.
- [17] Azam S.E., Bagherinia, M., Mariani, S., Stochastic system identification via particle and sigma-point Kalman filtering, *Scientia Iranica*, 19(4), 2012, 982–991.
- [18] Arulampalam S, Maskell S, Gordon N, Clapp T, A tutorial on particle filters for on-line non-linear/non-Gaussian, Bayesian tracking, *IEEE Transactions on Signal Processing*, 50(2), 2002, 174–188.
- [19] Azam, S.E., Ghisi, A., Mariani, S., Parallelized sigma-point Kalman filtering for structural dynamics, *Computers and Structures*, 92–93, 2002, 193–205.
- [20] Julier, S.J., Uhlmann, J.K., New Extension of the Kalman Filter to Nonlinear Systems, *Proceedings of SPIE 3068, Signal Processing, Sensor Fusion, and Target Recognition VI*, 182–193, 1997.
- [21] Merwe, R. Van Der, Wan, E., Sigma-point Kalman filters for integrated navigation, The Institute of Navigation, Oregon Health & Science University, 2004.
- [22] Wu, M., Smyth, A.W., Application of the unscented Kalman filter for real-time nonlinear structural system identification, *Structural Control and Health Monitoring*, 14(7), 2007, 971–990.
- [23] Mariani, S., Ghisi, A., Unscented Kalman filtering for nonlinear structural dynamics, *Nonlinear Dynamics*, 49(1–2), 2007, 131–150.
- [24] Erazo, K., Nagarajaiah, S., Bayesian structural identification of a hysteretic negative stiffness earthquake protection system using unscented Kalman filtering, *Structural Control and Health Monitoring*, 25(9), 2018, e2203.
- [25] Sen, D., Erazo, K., Nagarajaiah, S., Bayesian estimation of acoustic emissions source in plate structures using particle-based stochastic filtering, *Structural Control and Health Monitoring*, 24(11), 2017, e2005.
- [26] Li, L., Qin, H., An UKF-based nonlinear system identification method using interpolation models and backward integration, *Structural Control and Health Monitoring*, 25(4), 2017, e2129.
- [27] Yan, G., Sun, H., Büyüköztürk, O., Impact load identification for composite structures using Bayesian regularization and unscented Kalman filter, *Structural Control and Health Monitoring*, 24(5), 2017, e1910.
- [28] Noshirvani, G., Askari, J., Fekih, A., Fractional-order fault-tolerant pitch control design for a 2.5 MW wind turbine subject to actuator faults, *Structural Control and Health Monitoring*, 26(10), 2019, e2441.
- [29] Marafioti, G., Enhanced Model Predictive Control: Dual Control Approach and State Estimation Issues, Ph. D. Thesis, Department of Engineering Cybernetics, Norwegian University of Science and Technology, Trondheim, 2010.
- [30] Sunderhauf, N., Using the unscented Kalman filter in mono-SLAM with inverse depth parametrization for autonomous airship control, In Proc. of IEEE International Workshop on Safety Security and Rescue Robotics, Rome, Italy, 2007.
- [31] Wang, X. Nonlinear Control and Estimation with General Performance Criteria, Ph. D. Thesis, Department of Electrical and Computer Engineering, Marquette University, Milwaukee, WI, 2011.
- [32] Jacob, N.C., Dhib, R., Unscented Kalman filter based nonlinear model predictive control of a LDPE autoclave reactor, *Journal of Process Control*, 21(9),



- 2011, 1332–1344.
- [33] Araki, N., Okada, M., Parameter identification and swing-up control of an acrobot system, *IEEE Conference on Decision and Control and European Control Conference*, Hong Kong, China, 1040–1045, 2005.
- [34] Bisgaard, M., la Cour-Harbo, A., Dimon Bendtsen, J., Adaptive control system for autonomous helicopter slung load operations, *Control Engineering Practice*, 18(7), 2010, 800–811.
- [35] Wagg, D.J., Partial synchronization of non-identical chaotic systems via adaptive control, with applications to modelling coupled nonlinear systems, *International Journal of Bifurcation and Chaos*, 12(3), 2002, 561–570.
- [36] Miah, M.S., Chatzi, E.N., Dertimanis, V.K., Weber, F., Real-time experimental validation of a novel semi-active control scheme for vibration mitigation, *Structural Control and Health Monitoring*, 24(3), 2017, e1878.
- [37] Garces, F., Becerra, V.M., Kambhampati, C., Warwick, K., *Strategies for Feedback Linearisation: A Dynamic Neural Network Approach*, Springer-Verlag, London, 2003.
- [38] Isidori, A., *Nonlinear control systems*, 3<sup>rd</sup> Ed., Springer, New York, 1995.
- [39] Johnson, E., Erkus, B., Structural Vibration Mitigation Using Dissipative Smart Damping Devices, *IUTAM Symposium on Nonlinear Stochastic Systems*, Monticello, Illinois, USA, 227–236, 2003.
- [40] Rajamohan, V., Sedaghati, R., Rakheja, S., Optimal vibration control of beams with total and partial MR-fluid treatments, *Smart Materials and Structures*, 20(11), 2011, 115016.
- [41] Liu, X., Goldsmith, A., Kalman filtering with partial observation losses, *43<sup>rd</sup> IEEE Conference on Decision and Control*, Nassau, Bahamas, 4180–4186, 2004.
- [42] Levine, W., Athans, M., On the determination of the optimal constant output feedback gains for linear multivariable systems, *IEEE Transactions on Automatic Control*, 15(1), 1970, 44–48.
- [43] Hendrix, C.D., Veth, M.J., Carr, R.W., LQG control design for a hovering micro air vehicle using an optical tracking system, *2009 IEEE Aerospace Conference*, Montana, USA, 1–14, 2009.
- [44] Jimenez, A., Al-Hadithi, B., Matia, F., Extended Kalman Filter for the Estimation and Fuzzy Optimal Control of Takagi-Sugeno Model, in Grigorie, T.L. (Ed.), *Fuzzy Controllers, Theory and Applications*, Ch.4, IntechOpen, London, 2011.
- [45] Gawronski, W., *Modeling and control of antennas and Telescopes*, Springer Science+Business Media, LLC, Pasadena, 2008.
- [46] Miah, M.S., Chatzi, E.N., Weber, F., Semi-active control of structural systems with uncertainties using an unscented Kalman filter, in Zingoni, A. (Ed.), *Research and Applications in Structural Engineering, Mechanics and Computation*, CRC Press, Boca Raton, 2013.
- [47] Dertimanis, V.K., Chatzi, E.N., LQR-UKF active comfort control of passenger vehicles with uncertain dynamics, *IFAC-PapersOnLine*, 51(15), 2018, 120–125.
- [48] Dertimanis, V.K., Chatzi, E.N., Weber, F., LQR-UKF Semi-Active Control Of Uncertain Structures, In *EACS 2016-6th European Conference on Structural Control*, Sheffield, UK, #161, 2016.
- [49] Miah, M.S., Chatzi, E.N., Dertimanis, V.K., Weber, F., Real-time experimental validation of a novel semi-active control scheme for vibration mitigation, *Structural Control and Health Monitoring*, 24(3), 2017, e1878.
- [50] Mariani, S., Corigliano, A., Impact induced composite delamination: state and parameter identification via joint and dual extended Kalman filters, *Computer Methods in Applied Mechanics and Engineering*, 194(50–52), 2005, 5242–5272.
- [51] Konatowski, S., Kaniewski, P., Matuszewski, J., Comparison of Estimation Accuracy of EKF, UKF and PF Filters, *Annual of Navigation*, 23(1), 2016, 69–87.
- [52] Chatzi, E.N., Smyth, A.W., Masri, S.F., Experimental application of on-line parametric identification for nonlinear hysteretic systems with model uncertainty, *Journal of Structural Safety*, 32(5), 2010, 326–337.
- [53] Dertimanis, V.K., Chatzi, E.N., Eftekhar Azam, S., Papadimitriou, C., Input-state-parameter estimation of structural systems from limited output information, *Mechanical Systems and Signal Processing*, 126, 2019, 711–746.
- [54] Wagg, D., Neild, S., *Nonlinear Vibration with Control*, Springer International Publishing, Basel, 2015.
- [55] Anderson, B.D.O., Moore, J.B., *Optimal Control Linear Quadratic Methods*, Prentice-Hall Inc., Englewood Cliffs, 1989.
- [56] Miah, M.S., Chatzi, E.N., Weber, F., Semi-active control for vibration mitigation of structural systems incorporating uncertainties, *Smart Materials and Structures*, 24(5), 2015, #055016.
- [57] Lublin, L., Athans, M., Linear Quadratic Regulator Control, in Levine, W.S. (Ed.), *The Control Handbook*, 2<sup>nd</sup> Ed., Vol.3, Ch. 17, CRC Press, Boca Raton, 2011.
- [58] Cebon, D., *Handbook of Vehicle-Road Interaction*, Swets & Zeitlinger, Lisse, 2000.
- [59] Asgarieh, E., Moaveni, B., Barbosab, A.R., Chatzi, E., Nonlinear model calibration of a shear wall building using time and frequency data features, *Mechanical Systems and Signal Processing*, 85, 2017, 236–251.
- [60] Julier, S.J., Uhlmann, J.K., Consistent Debaised Method for Converting Between Polar and Cartesian Coordinate Systems, *Proceedings of SPIE 3086, Acquisition, Tracking, and Pointing*, 1997.
- [61] Chatzi, E. N., Smyth, A.W., Nonlinear System Identification: Particle based methods, in: Beer M., Patelli E., Kougioumtzoglou I., Au I. (Ed.) *Encyclopedia of Earthquake Engineering*, Springer-Verlag, Berlin Heidelberg, 2014.
- [62] Chatzi, E.N., Smith, A.W., Particle filter scheme with mutation for the estimation of time-invariant parameters in structural health monitoring applications, *Structural Control and Health Monitoring*, 20, 2013, 1081–1095.
- [63] Chatzi, E., Smyth, A.W., The unscented Kalman filter and particle filter methods for nonlinear structural system identification with non-collocated heterogeneous sensing, *Structural Control and Health Monitoring*, 16(1), 2009, 99–123.

## ORCID iD

Vasilis K. Dertimanis  <https://orcid.org/0000-0002-4671-1962>  
 Eleni N. Chatzi  <https://orcid.org/0000-0002-6870-240X>  
 Sami F. Masri  <https://orcid.org/0000-0001-5856-4456>



© 2021 Shahid Chamran University of Ahvaz, Ahvaz, Iran. This article is an open access article distributed under the terms and conditions of the Creative Commons Attribution-NonCommercial 4.0 International (CC BY-NC 4.0 license) (<http://creativecommons.org/licenses/by-nc/4.0/>).

How to cite this article: Dertimanis V.K., Chatzi E.N., Masri S.F. On the Active Vibration Control of Nonlinear Uncertain Structures, *J. Appl. Comput. Mech.*, 7(SI), 2021, 1183–1197. <https://doi.org/10.22055/JACM.2020.34007.2322>

